Registration of Point-Clouds from Terrestrial Laser Scanners and Portable Laser Scanners

Takuma Watanabe[*1], **Takeru Niwa**[*2], **and Hiroshi Masuda**[*3]

[*1] The University of Electro-Communications, 1-5-1 Chofugaoka, Chofu, Tokyo 182-8585
E-mail: takuma.watanabe@uec.ac.jp
[*2] The University of Electro-Communications, 1-5-1 Chofugaoka, Chofu, Tokyo 182-8585
E-mail: takeru.niwa@uec.ac.jp
[*3] The University of Electro-Communications, 1-5-1 Chofugaoka, Chofu, Tokyo 182-8585
E-mail: h.masuda@uec.ac.jp

Abstract. We propose a registration method for point-clouds that are captured using a terrestrial laser scanner (TLS) and a portable laser scanner (PLS). Since a portable laser scanner covers a very limited region, sufficient cues for registration are often missing. In our method, the system analyses large-scale point-clouds, which are captured using a TLS, and indicates candidate regions to be measured using a PLS. When the user measures a suggested region, the system aligns a point-cloud captured using a short-range point-cloud to a large-scale point-cloud. Our experiments show that our registration method can adequately align point-clouds captured using a TLS and a PLS.

Keywords: registration, 3D scanning, point-cloud

1. INTRODUCTION

Engineering facilities and infrastructures require maintenance and renovation repeatedly because of their aged deterioration. It is well known that the efficiency of maintenance can be improved using computer simulation based on 3D models. However, there are no 3D models of old facilities in most cases. Even when there are 3D models, the aged deterioration and distortion are not represented on 3D models of engineering facilities.

Terrestrial laser scanners (TLS) are useful to capture as-is 3D shapes of components in facilities. The TLS is a powerful tool to measure large fields, because measurement ranges are very long. The state-of-the-art TLS can capture tens of million points within 100 m in a minute.

However, the resolutions of TLSs are not sufficient to measure detail shapes of deterioration. Typical resolutions of high-performance TLSs are 6 mm at the distance of 10m, and the resolutions further decline at far distance. Therefore, deterioration such as corrosion cannot be captured using TLSs. In addition, when there are a lot of components in facilities, many components are occluded by other components. Occluded portions are missing from point-clouds. This problem is partly caused because TLSs cannot be placed in small spaces.

On the other hand, portable laser scanners (PLS) can capture detail shapes in high resolutions. They are useful to measure aged deterioration and distortion of components. However, the measurement ranges of PLSs are very limited and are not suitable to measure a wide range of fields.

It is useful to generate point-clouds that represent wide fields of engineering plants and partly have detail shapes. Therefore, we consider to complement missing portions or detail shapes with point-clouds captured using a PLS. In this research, we use a TLS, which can measure in the distance of more than 100m, and a PLS, which can measure only within 23cm. We refer point-clouds captured using a TLS as *large-scale point-clouds*, and point-clouds captured using a PLS as *short-range point-clouds*.

In this paper, we discuss registration of a large-scale point-cloud and short-range point-clouds. Registration is one of the most fundamental techniques in point processing. So far, many registration methods have been

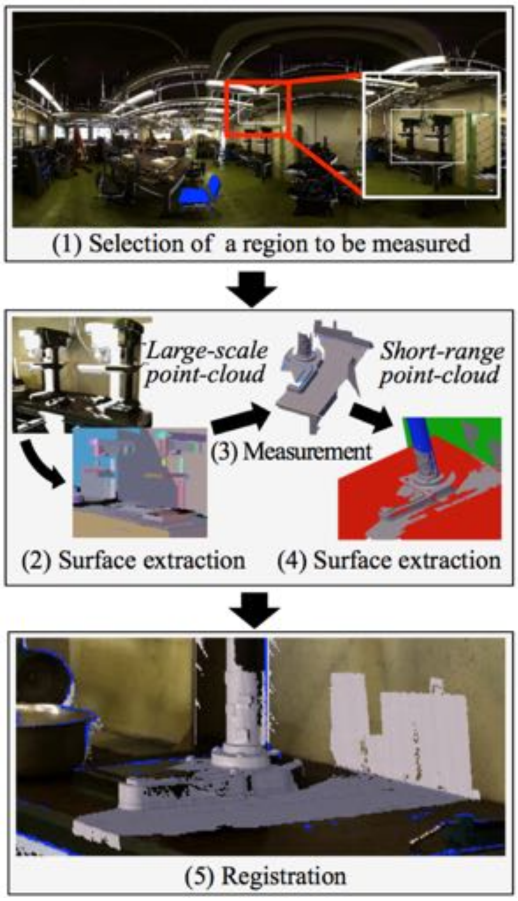

Fig. 1 Our approach for registration of point-clouds

proposed [1-19]. However, conventional methods do not assume that the resolutions and scales of two point-clouds are enormously different. Especially, when a point-cloud covers only a very small region, registration is almost impossible because there are very few cues for matching positions.

Our approach is shown in **Fig. 1**. First the user specifies a region in a large-scale point-cloud. Then the system detects planes and cylinders from a large-scale point-cloud, and suggests a combination of surfaces that are suitable for registration of short-range point-clouds. If the user measures suggested surfaces using a PLS as well as the region of interest, the system aligns the short-range point-clouds to a large-scale point-cloud.

In the following section, we explain a TLS and a PLS, which are used in this research. In Section 3, we describe an overview of our registration method. In Section 4, surface extraction is explained. In Section 5, we describe details of our registration method. Then we show experimental results in Section 6, and finally we conclude our research.

2. LASER SCANNERS

2.1. Terrestrial Laser Scanner

TLSs can capture dense point-clouds from a large-scale engineering facility. The terrestrial laser scanner emits a laser beam to an object and measure the round-trip travel time of the laser beam. As shown in **Fig. 2**, the directions of laser beams are vertically shifted by the spinning miller and horizontally moved by the rotating base. In this research, we used a HDS7000 (Leica Geosystems), which is a phase-shift type of laser scanner. This scanner can capture up to 1,016,727 points per second. The maximum measurable distance is 187 m. **Fig. 3** shows an example of point-clouds captured by this scanner.

2.2. Portable Laser Scanner

PLSs can capture more detail and precise point-clouds than TLSs. In this research, we use a hand-held 3D scanner P3D NC-2323S (Nikon), as shown in **Fig. 4**. **Table 1** shows the specification of P3D NC-2323S. Although the measurement error is very small, the measurement range is only 23 cm. This scanner measures objects using a tripod or in a hand-held manner. When the user measures an object at different positions, the user is required to measure it so that measurement ranges are overlapped. Then post-process software automatically registers point-clouds sequentially. In this research, we suppose that short-range point-clouds that are measured successively are represented using the common coordinate system.

Fig. 5 shows a mesh model generated from short-range point-clouds. Since the measurement error is less than 0.3mm, the degradation of the metal surface is clearly represented on this model.

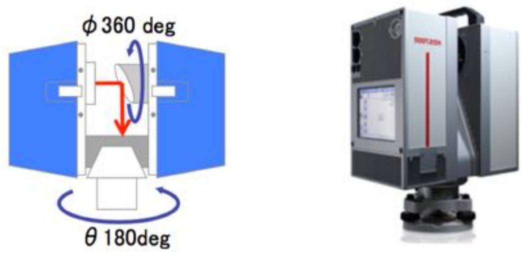

(a) Mechanism of TLS (b) HDS 7000

Fig. 2 Terrestrial laser scanner

Fig. 3 An example of a large-scale point-cloud

3. REGISTRATION SCHEME

When a short-range point-cloud is aligned to a large-scale point-cloud, six degrees-of-freedom, which consist of three translational and three rotational parameters, have to be uniquely determined. Therefore, short-range point-clouds have to include enough points to determine the six degrees-of-freedom. For example, when a short-range point-cloud consists of only a planar surface, two translational and one rotational degrees-of-freedom cannot be determined.

In our method, planes, cylinders, and straight boundary edges are extracted from point-clouds, and they are used for registration. Short-range point-clouds are aligned to a large-scale point-cloud by aligning coincident surfaces or straight edges.

As shown in **Fig. 6**, there are eight schemes to fix all six degrees-of-freedom using planes, cylinders, and boundary straight edges. When both of the short-range point-cloud and the large-scale include surfaces or edges in one of the eight schemes, short-range point-clouds can be uniquely registered to the large-scale point-cloud.

(a) Tripod (b) Hand-held

Fig. 4 Nikon P3D NC-2323S

Table. 1 Specification of P3D

Weight	1.9 kg
Size	180 × 260 × 50 mm
Measuring Point	1024 × 1024 (max)
Measuring Range	230 × 230 mm, Z = ±50 mm
Maximum Error	0.3 mm

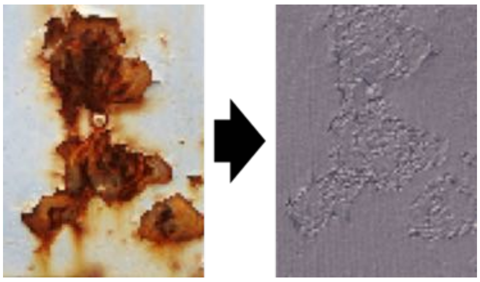

(a) Metal surface (b) 3D model

Fig. 5 Corrosion measured by a portable laser scanner

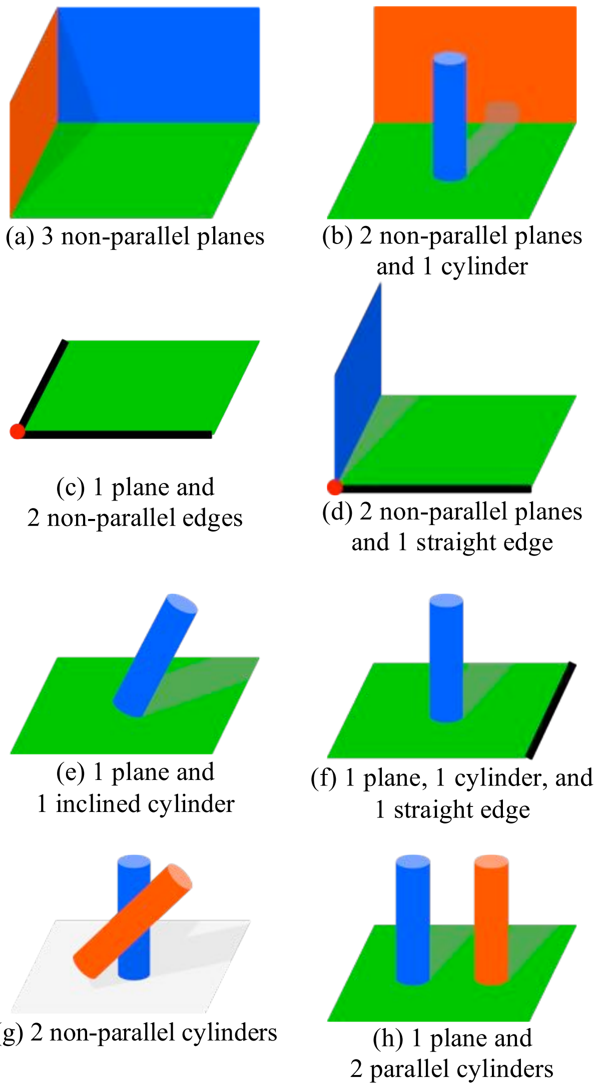

(a) 3 non-parallel planes
(b) 2 non-parallel planes and 1 cylinder
(c) 1 plane and 2 non-parallel edges
(d) 2 non-parallel planes and 1 straight edge
(e) 1 plane and 1 inclined cylinder
(f) 1 plane, 1 cylinder, and 1 straight edge
(g) 2 non-parallel cylinders
(h) 1 plane and 2 parallel cylinders

Fig. 6 Eight registration schemes based on planes, cylinders, and straight boundary edges

4. Extraction of Surfaces and Edges

In our registration method, planes, cylinders, and boundary straight edges are used for registration. Therefore, surfaces and straight edges have to be extracted from point-clouds.

To extract planes and cylinders, we use the method proposed by Masuda, et al. [20]. In this method, surfaces are extracted using the RANSAC method for point-clouds [21]. The RANSAC method is very time-consuming when it is applied to large-scale point-clouds. Therefore, Masuda, et al. recursively subdivided a point-cloud and restricted search regions for the RANSAC method. **Fig. 7** shows planes and cylinders that were extracted from a large-scale point-cloud using this method. When planar and cylindrical regions are detected, surface equations can be calculated using the least-square method [22,23].

We also extract boundary straight edges. When a planar region is detected, the boundary points are extracted from the points in the planar region. Straight lines can be detected using the RANSAC method. As shown in **Fig. 8**(a), two points are randomly selected from boundary points, and a straight line through the two points is calculated. Then the number of points on the straight line is counted. The system repeats this process many times, and selects a straight line that the number of points is largest. When a straight line is detected, points on the straight line are eliminated from the boundary points, and other straight lines are searched for. **Fig. 8**(b) shows detected straight lines on a planar region.

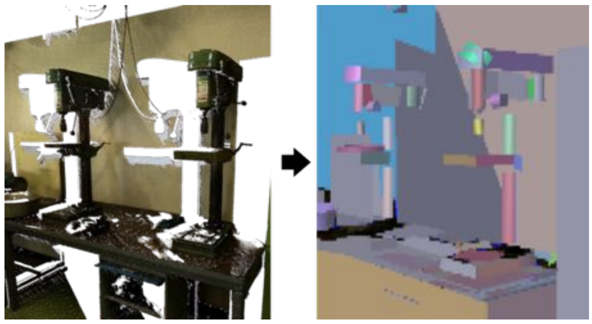

(a) Large-scale point-cloud (b) Planes and cylinders

Fig. 7 Extraction of planes and cylinders

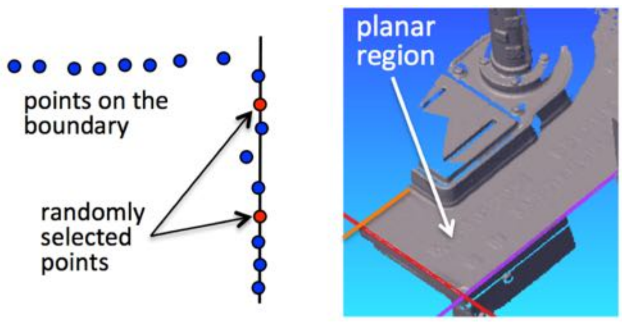

(a) RANSAC method (b) Detected straight lines

Fig. 8 Extraction of boundary straight edges

5. REGISTRATION OF POINT-CLOUDS

5.1. Registration Method

We propose a registration method for point-clouds captured using a TLS and a PLS. Since a PLS covers a very limited region, cues to determine the six degrees-of-freedom are often missing. Therefore, our method suggests candidate regions to be measured using a PLS so that a registration matrix can be uniquely calculated.

In our system, a large-scale point-cloud is displayed on a screen, and the user draws a square on the screen, as shown in **Fig. 9**, so that sufficient cues for registration are included in the square as well as a region of interest.

In our method, planes and cylinders are used as cues for registration. All planes and cylinders are extracted from a large-scale point-cloud and stored in a preprocess phase, as shown in **Fig. 10**. When the user specifies a square region, the system selects planes and cylinders in the selected region, and suggests possible combinations of surfaces.

Fig. 9 Specification of a square region

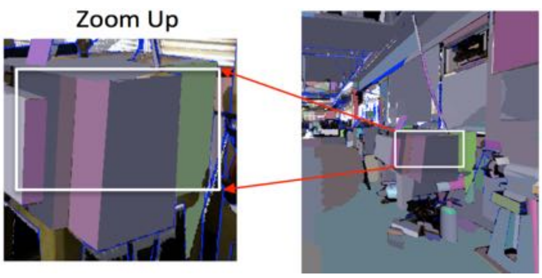

Fig. 10 Selection of Surfaces to be measured

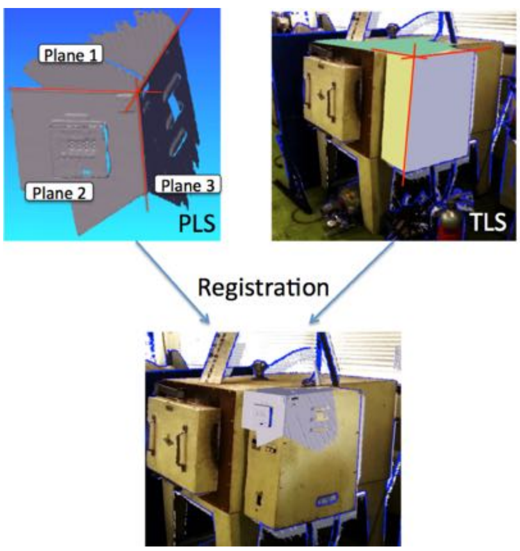

Fig. 11 Registration of point-clouds

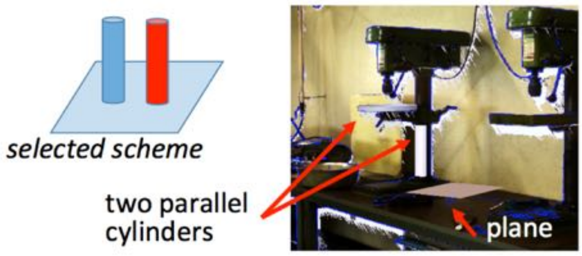

(a) Selection of a scheme and surfaces

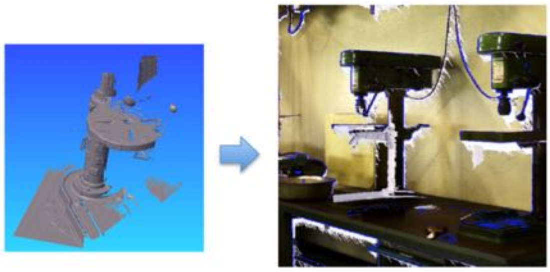

(b) Registration of a short-range point-cloud

Fig. 12 Registration using a plane and cylinders

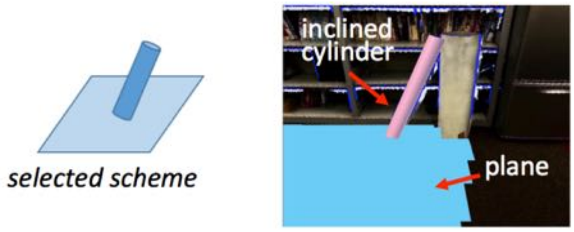

(a) Selection of a scheme and surfaces

(b) Registration of a short-range point-cloud

Fig. 13 Registration using a plane and a cylinder

The user is required to measure the suggested surfaces to complete registration. When short-range point-clouds are captured using a PLS, the system extracts surfaces and straight edges and applies our registration method to point-clouds, as shown in **Fig. 11**.

Corresponding surfaces or edges are aligned using one of eight schemes shown in Fig. 6. Therefore, it is necessary to determine which scheme is selected and which surfaces and edges are used for registration.

In our system, we implemented two modes. In a manual mode, the user selects a scheme and specifies surfaces or edges in a large-scale point-cloud on a screen. In an automatic mode, the system automatically estimates the optimal combination of surfaces and edges using large-scale and short-range point-clouds.

Examples of manual selections are shown in **Fig. 12** and **Fig. 13.** In Fig. 12, the user selects the scheme of two parallel cylinders and a plane, and specifies two cylinders and a plane in a large-scale point-cloud. Then the system extracts corresponding surfaces from a short-range point-cloud, calculates a registration matrix, and aligns a short-range point-cloud to a large-scale point-cloud, as shown in Fig. 12(b). In Fig. 13, the user specifies the scheme of a plane and an inclined cylinder, and selects a plane and a cylinder in a large-scale point-cloud. The registered point-clouds are shown in Fig. 13(b).

5.2. Automatic Selection of Registration Schemes

In an automatic mode, the system automatically estimates the optimum scheme. **Fig. 14** shows a process of automatic registration.

When two point-clouds captured using a TLS and a PLS are given, the system detects surfaces from each point-cloud and selects possible schemes in eight ones. Since surfaces can be more robustly extracted than straight edges, combinations with only surfaces are selected in priority to ones with straight edges.

Then the system estimates corresponding surfaces or straight edges. Suppose that a scheme consists of α surfaces and β straight edges. When s_1 surfaces and e_1 straight edges are detected in a large-scale point-cloud, and s_2 surfaces and e_2 straight edges in a short-range point-cloud, the number of possible combinations is

$$({}_{s1}P_{\alpha} \times {}_{e1}P_{\beta})\times({}_{s2}P_{\alpha} \times {}_{e2}P_{\beta}).$$

Since it is time-consuming to evaluate all combinations, we reduce candidates using normal vectors of planes and directional vectors of cylinder axes. As shown in **Fig. 15**, when corresponding surfaces are aligned, differences between vectors are calculated. When the sum of differences is less than a threshold, the corresponding pairs are accepted.

Then we further evaluate whether points in two point-clouds are consistent. In this process, points on surfaces in a short-range point-cloud are transformed onto a large-scale point-cloud, and distances between points and surfaces are evaluated, as shown in **Fig. 16**. When the distance of a point is less than a threshold, the point is regarded as a consistent point. We denote the number of points on planes in a short-range point-cloud as N_p, and the number of consistent points as N_c. We accept a registration matrix when the following formula is satisfied.

$$\frac{N_c}{N_p} > \delta$$

Otherwise, the registration matrix is rejected. In this research we specified $\delta = 0.5$. When multiple candidates satisfy this criterion, the combination with the maximum N_c is selected.

To reduce computation time, we process this evaluation in two steps. In the first step, a small number of points are selected from a short-range point-cloud and they are used for evaluation. When the first evaluation result is accepted, all points on surfaces are evaluated in the second step.

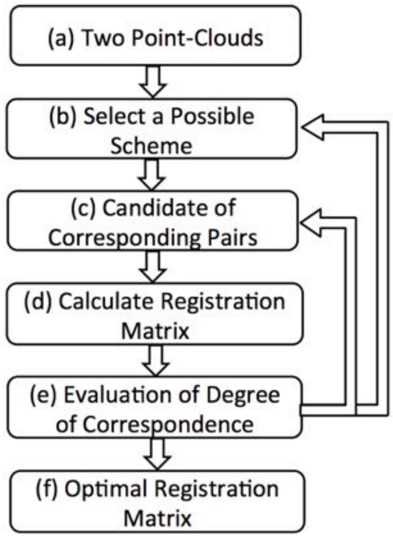

Fig. 14 Process of registration

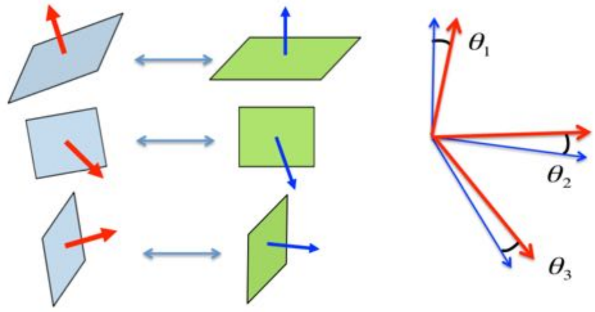

(a) Short-range (b) Large-scale (c) Differences

Fig. 15 Evaluation of corresponding vectors

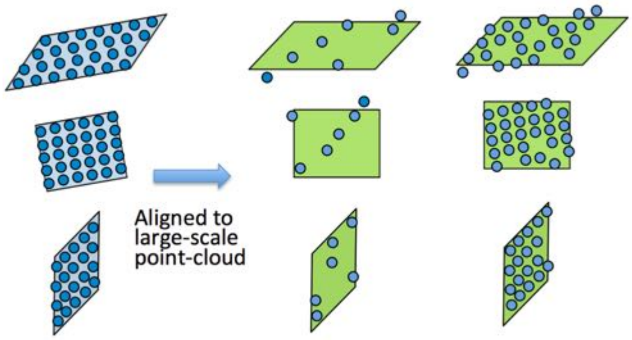

(a) Short-range points (b) Rejected (c) Accepted

Fig. 16 Evaluation of consistency of points

5.3. Merging Point-Clouds

When two point-clouds are aligned, we merge the two point-clouds by eliminating overlapped points in a large-scale point-cloud. This process is required to avoid that detail short-range point-clouds are occluded by a sparse large-scale point-cloud. Overlapping portions are detected on a panorama image, which is generated using a large-scale point-cloud. A panorama image can be generated by converting all (x, y, z) coordinates of points into spherical coordinates (θ, ϕ, r), and quantizing angles (θ, ϕ) into integer coordinates (i, j).

Overlapping portions can be detected by projecting a short-range point-cloud onto the panorama image, as shown in **Fig. 17**. When the difference between two points on the same pixel is less than a threshold, the points are regarded as overlapping and removed from a large-scale point-cloud.

When overlapping points are eliminated, boundaries of overlapping portions may become discontinuous because of registration errors, as shown in **Fig. 18**(a). Therefore, we blend overlapping points near boundaries. We suppose that $\mathbf{p}_l$ in a large-scale point-cloud and $\mathbf{p}_s$ in a short-range point-cloud are overlapping. Then the blended coordinate is calculated as:

$$\{d\mathbf{p}_l + (D-d)\mathbf{p}_s\}/D$$

where d is the distance from the boundary of overlapping portions, and D is the blending width defined by the user. **Fig. 18**(b) shows a blended result, in which gaps are interpolated between two point-clouds.

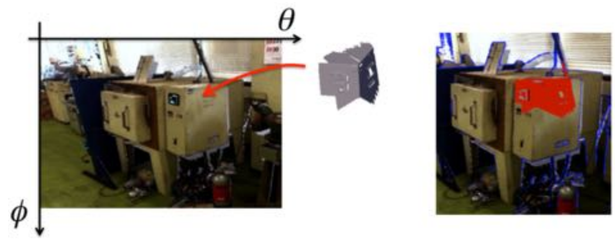

(a) Panorama image (b) Overlapping region

Fig. 17 Detection of overlapping portions

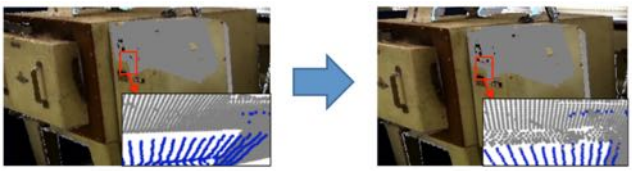

(a) Small gap at boundary (b) Blended boundary

Fig. 18 Blending coordinates near boundaries

6. Experiment and Results

We evaluated our method using an actual point-cloud of an engineering plant. CPU time was measured using a desktop PC with 3.10 GHz Intel Core i5 and 16.0 GB RAM. The scanner for large-scale point-clouds was Leica-Geosystems HDS7000. The scanner for short-range point-clouds was Nikon P3D NC-2323S.

To evaluate eight schemes for registration, we selected examples in which eight schemes are included. **Fig. 19** shows the examples of point-clouds. Then we measured appropriate regions using a PLS, and applied our registration method to the point-clouds. In this experiments, we specified a scheme for each example, and selected sufficient planes and cylinders. When straight edges are involved in the scheme, the longest straight edges are automatically selected and used for registration.

In this evaluation, all short-range point-clouds could be successfully aligned to the large-scale point-clouds, as shown in **Fig. 19**.

We evaluated precision of registration results using a partial point-cloud shown in **Fig. 17**. We aligned a short-range point-cloud to a large-scale point-cloud, and calculated distances between points in a short-range point-cloud and planes in a large-scale point-cloud. In this experiment, the average distance was 1.2 mm, and the average angle between normal vectors of aligned planes was 0.81 degree.

Then we evaluated calculation time. In an automatic mode, the user selects a square region on a screen, and then a registration matrix is automatically calculated. When many planes or cylinders are included in the selected region, many combinations of surfaces have to be processed to obtain the optimum result. We reduced candidates in a pre-process phase. In **Table 2**, we show calculation time of three examples to confirm the efficiency of our pre-process. As shown in this table, it was time-consuming when all combinations of surfaces were calculated. On the other hand, our method with the pre-process for reducing combinations could significantly reduce a calculation time.

Table. 2 Calculation time

	Number of Surfaces		Number of Combinations		CPT Time (sec)	
	Large-Scale	Short-Range	All	Pre-Processed	All	Pre-Processed
Case 1	8	4	1344	115	1.1	0.09
Case 2	12	4	5280	202	10.5	0.4
Case 3	8	7	11760	951	26.0	2.1

7. Conclusion

We presented a registration method for aligning short-range point-clouds captured using a PLS to a large-scale point-cloud captured using a TLS. We introduced eight registration schemes based on planes, cylinders, and straight edges. We evaluated our method and we showed that eight schemes could successfully align point-clouds. In addition, we showed that our method could align point-clouds in a reasonable time and precision.

In future work, we would like to evaluate precision in more cases, because we evaluated our method using a single large-scale point-cloud. We proposed eight schemes, but did not discuss their priority sequence. We would like to investigate which schemes are better than others.

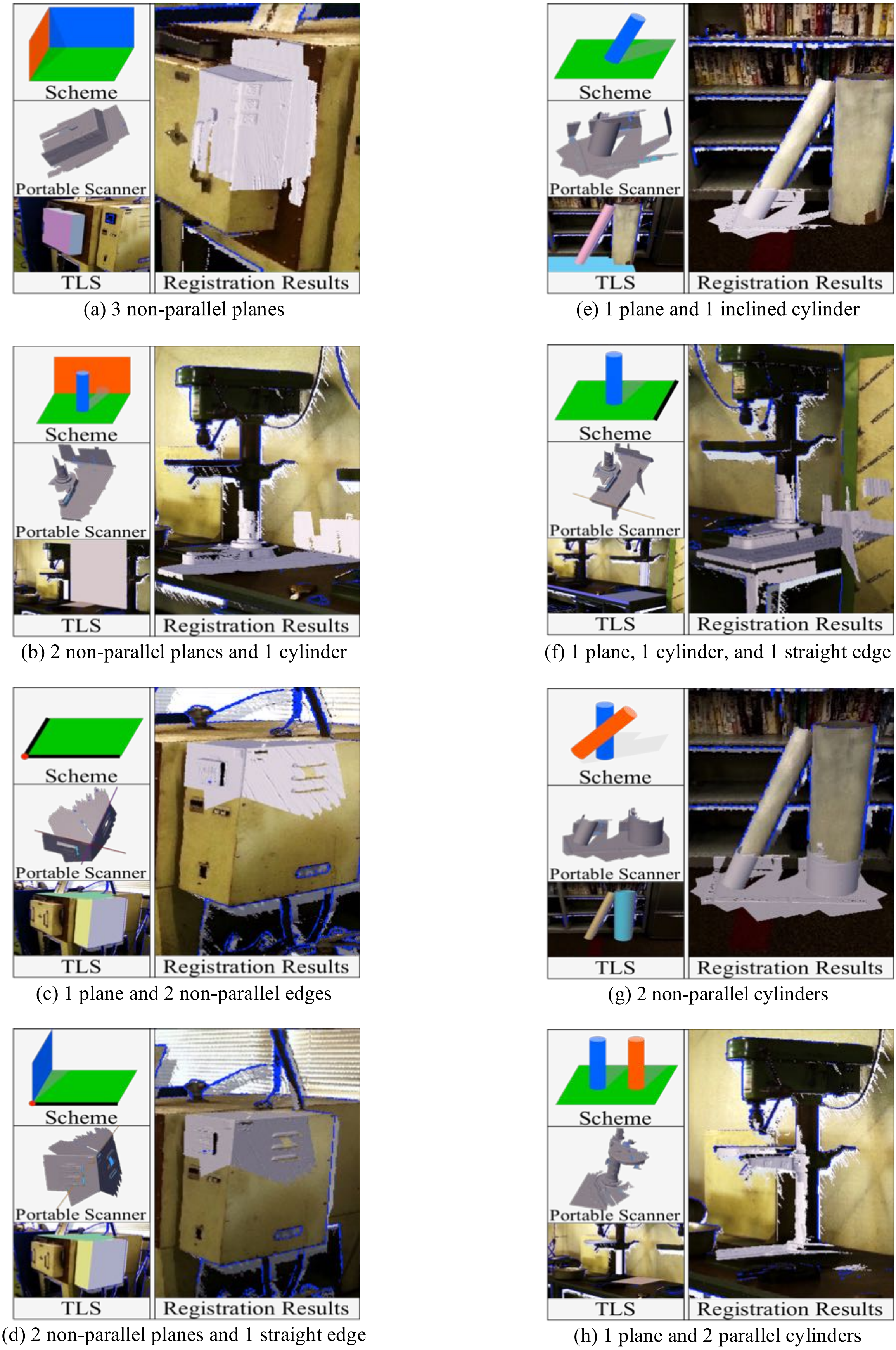

(a) 3 non-parallel planes

(e) 1 plane and 1 inclined cylinder

(b) 2 non-parallel planes and 1 cylinder

(f) 1 plane, 1 cylinder, and 1 straight edge

(c) 1 plane and 2 non-parallel edges

(g) 2 non-parallel cylinders

(d) 2 non-parallel planes and 1 straight edge

(h) 1 plane and 2 parallel cylinders

Fig. 19 Experimental Results

Acknowledgements

We would like to thank to Nikon Corp. for providing the hand-held 3D scanner P3D NC-2323S.

REFERENCES:

[1] P. J. Besl, and N. D. Mckay, “A method for registration of 3-D shapes,” IEEE Transactions on Pattern Analysis and Machine Intelligence, vol. 14, pp. 239-256, February 1992.

[2] S. Rusinkiewicz, and M. Levoy, “Efficent cariants of the ICP algorithm,” 3-D Digital Imaging and Modeling, 2001. Proceedings. Third International Coference on IEEE, pp. 145-152, 2001.

[3] R.B.Rusu, N. Blodow, and M. Beetz, “Fast point feature histograms (FPFH) for 3D registration,” Robotics and Automation, ICRA'09. IEEE International Conference, pp.3212-3217, May 2009.

[4] H. Men, B. Gebre, and K. Pochiraju, “Color point cloud registration with 4D ICP algorithm”, Robotics and Automation (ICRA), 2011 IEEE International Conference on. IEEE, pp. 1511-1516, 2011.

[5] J. Chen, X. Wu, M. Y. Wang, and X. Li, “3D shape modeling using a self-developed hand-held 3D laser scanner and an efficient HT-ICP point cloud registration algorithm.” Optics & Laser Technology, vol. 45, pp.414-423, 2013.

[6] N. J. Mitra, N. Gelfand, H. Pottmann, and L. Guibas, “Registration of point cloud data from a geometric optimization perspective,” Proceedings of the 2004 Eurographics/ACM SIGGRAPH symposium on Geometry processing, pp. 22-31, July 2004.

[7] I. Stamos, and M. Leordean, “Automated feature-based range registration of urban scenes of large scale,” Computer Vision and Pattern Recognition, 2003 Proceedings. 2003 IEEE Computer Society Coference, vol. 2, pp.555-561, June 2003.

[8] J. L. Martinez, A. J. Reina, J. Morales, A. Mandow, and A. J. Garcia-Cerezo, “Using multicore processors to parallelize 3D point cloud registration with the Coarse Binary Cubes method,” Mechatronics (ICM), 2013 IEEE International Conference, pp.335-340, February 2013.

[9] J. Liu, G. Geng, and M. Zhou, "Sequence Iterative 3D Registration of Multi-view Point Cloud for Cultural Site Scenes," Computer Science & Service System (CSSS), 2012 International Conference on. IEEE, pp.1923-1927, Augast 2012.

[10] L. Jun, L. Wei, D. Donglai, and S. Qiang, “Point cloud registration algorithm based on NDT with variable size voxel,” Control Conference, 2015 34th Chinese, IEEE, pp. 3707-3712, July 2015.

[11] J. Jiang, J. Cheng, X. Chen, “Registration for 3-D point cloud using angular-invariant feature,” Neurocomputing, vol.72, pp.3839-3844, October 2009.

[12] T. T. Tran, V. T. Cao, D. Laurendeau, “3D point cloud registration based on the vector field representation.” Pattern Recognition (ACPR), 2013 2nd IAPR Asian Conference on. IEEE, pp.491-495, November 2013.

[13] A.Makadia, A.Patterson, K.Dainiilidis, “Fully automatic registration of 3D point clouds,” Computer Vision and Pattern Recognition, vol. 1, pp.1297-1304, June 2006.

[14] J. Y. Han, N. H. Perng, and H. J. Chen, “LiDAR point cloud registration by image detection technique.” Geoscience and Remote Sensing Letters, IEEE, vol. 10.4, pp. 746-750, November 2012.

[15] D. Grant, J. Bethel, and M. Crawford, “Point-to-plane registration of terrestrial laser scans” ISPRS Journal of Photogrammetry and Remote Sensing, vol. 72, pp.16-26, August 2012.

[16] J. Xiao, B. Adler, J. Zhang, and H. Zhang, “Planar Segment Based Three‐dimensional Point Cloud Registration in Outdoor Environments” Journal of Field Robotics, vol. 30.4, pp.552-582, July 2013.

[17] N. Li, P. Cheng, M. A. Sutton, and S. R. McNeill, “Three-dimensional point cloud registration by matching surface features with relaxation labeling method.” Experimental mechanics, vol. 45.1, pp. 71-82, 2005

[18] B. Yang, and Y. Zang, “Automated registration of dense terrestrial laser-scanning point clouds using curves.” ISPRS Journal of Photogrammetry and Remote Sensing, vol. 95, pp.109-121, September 2014.

[19] P. W. Theiler, and K. Schindler, “Automatic registration of terrestrial laser scanner point clouds using natural planar surfaces.” ISPRS Ann. Photogramm. Remote Sensing and Spatial Information Sciences, vol. 1, pp.173-178, 2012

[20] H. Masuda, T. Niwa, I. Tanaka, R. Matsuoka, “Reconstruction of Polygonal Faces from Large-Scale Point-Clouds of Engineering Plants,” Computer-Aided Design and Applications, vol. 12, pp. 555-563, April 2015.

[21] R. Schnabel, R. Wahl, R. Klein, “Efficient RANSAC for Point-Cloud Shape Detection, “ Computer Graphics Forum, vol. 26, no. 2, pp. 214-226, 2007.

[22] G. Lukacs, A.D. Marshall, R.R. Martin, “Faithful Least-Squares Fitting of Spheres, Cylinders, Cones and Tori for Reliable Segmentation,” Proceedings, 5th European Conference on Computer Vision, pp. 671–686, 1998.

[23] H. Masuda, I. Tanaka, “Extraction of Surface Primitives from Noisy Large-Scale Point-Clouds,” Computer-Aided Design and Applications, vol. 6, no. 3, pp.387-398, 2009.